Hindawi Publishing Corporation
Advances in Materials Science and Engineering
Volume 2014, Article ID 654012, 8 pages
http://dx.doi.org/10.1155/2014/654012

*Research Article*

# Nonlinear Finite Element Analysis of the Fluted Corrugated Sheet in the Corrugated Cardboard

**Zhiguo Zhang,[1,2,3] Tao Qiu,[2] Riheng Song,[2] and Yaoyu Sun[2]**

[1] *Department of Polymer Science and Engineering, Zhejiang University, Hangzhou, Zhejiang 310027, China*
[2] *School of Light Industry, Zhejiang University of Science and Technology, Hangzhou, Zhejiang 310023, China*
[3] *Shengda Group Co., Ltd, Hangzhou, Zhejiang 311264, China*

Correspondence should be addressed to Zhiguo Zhang; 107023@zust.edu.cn

Received 3 February 2014; Revised 20 May 2014; Accepted 21 May 2014; Published 23 July 2014

Academic Editor: Jun Zhang



The choice of corrugated medium, flute size, combining adhesive, and linerboards can be varied to design a corrugated board with specific properties. In this paper, the nonlinear finite element analysis of the fluted corrugated sheet in the corrugated cardboard based on software SolidWorks2008 was investigated. The model of corrugated board with three or more flutes is reliable for stress and displacement measurement to eliminate the influence of the number of flutes in models. According to the static pressure test, with the increase of flute height $H$ or arc radius of flute, the maximum stress in the models decreased and the maximum displacement increased. However the maximum stress and maximum displacement in the models increase nonlinearly in the static pressure test with the increase of the flute angle $\theta$. According to the drop test, with the increase of flute height $H$, the maximum stress of goods on the upper board in the drop test decreased. The maximum stress of the model in the drop test decreases firstly and then increases with the increase of flute angle, and the optimal flute angle $\theta$ could be 60° for corrugated board. All the conclusions are consistent with experimental data or product standards.

## 1. Introduction

Corrugated containers are the most important structural application of paperboard. Corrugated cardboard is a paper-based material consisting of a fluted corrugated sheet and one or two flat linerboards. It is widely used in the manufacture of corrugated cardboard boxes and shipping containers. The corrugated medium is often 0.026 pounds per square foot (0.13 kg/m$^2$) basis weight in the USA; in the UK, a 90 grams per square metre (0.018 lb/sq ft) fluting paper is common. At the single-facer, it is heated, moistened, and formed into a fluted pattern on geared wheels. This is joined to a flat linerboard with a starch based adhesive to form single face board. At the double-backer, a second flat linerboard is adhered to the other side of the fluted medium to form single wall corrugated board. Linerboards are test liners (recycled paper) or kraft paperboard (of various grades). The liner may be bleached white, mottled white, colored, or preprinted [1–3]. The basic geometry of typical twin corrugated wall board is illustrated in Figure 1.

Common flute sizes are "A," "B," "C," "E," and "F." The letter designation relates to the order that the flutes were invented, not the relative sizes. Flute size refers to the number of flutes per linear foot, although the actual flute dimensions for different corrugator manufacturers may vary slightly. Measuring the number of flutes per linear foot is a more reliable method of identifying flute size than measuring board thickness, which can vary due to manufacturing conditions. The most common flute size in corrugated cardboard boxes is "C" flute. The choice of corrugated medium, flute size, combining adhesive, and linerboards can be varied to engineer a corrugated board with specific properties to match a wide variety of potential uses.

The structural performance of a corrugated container is a function of numerous factors including the quality of the input cellulose fibers, the mechanical properties of the liner and medium, and the structural properties of the combined board. The complicated nonlinear behavior or paper makes modeling of the mechanical response of corrugated board

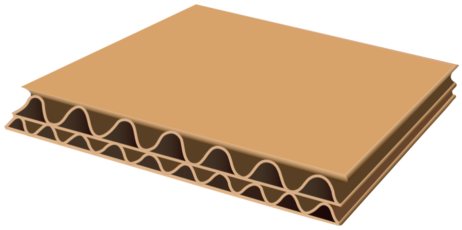


Figure 1: Twin corrugated wall board structure.

and structures composed of corrugated board a difficult task [4].

Numerous studies have been focused on the properties of corrugated cardboard and external environment's effects on the performance of corrugated carton [5–10]. Gilchrist et al. [4] have developed nonlinear finite element models for corrugated board configurations. Results from the finite element simulations correlated reasonably well with the analogous experimental measurements performed using actual corrugated board specimens. Biancolini and Brutti [11] have developed a finite element "corrugated board" by means of a dedicated homogenization procedure in order to investigate the buckling of a complete package. The FEM model of the package, assembled with this new element, can accurately predict the experimental data of incipient buckling observed during the standard box compression test, despite the few degrees of freedom and the minimal computational effort. Biancolini [12] also presented a numerical approach to evaluating the stiffness parameters for corrugated board. The method is based on a detailed micromechanical representation of a region of corrugated board modelled by means of finite elements. Conde et al. [13] have developed a methodology for modelling corrugated board adhesive joints subjected to shear, considered to be the main load in most of these joints. The corrugated board adhesive joint model reproduced quite well the stiffness obtained in the test samples, as well as the failure load with a deviation of less than 14%.

Biancolini et al. [1] compared results obtained from the simplified formula, an extended formula, and two numerical models developed by authors using finite elements (FE): an FE model realised with homogenised elements and an FE model representing the entire corrugation geometry. Numerical results of the capability to resist stacking loads obtained with FE models were consistent with experimental results. Haj-Ali et al. [14] presented a refined nonlinear finite element modeling approach for analyzing corrugated cardboard material and structural systems. This method can accurately predict overall mechanical behavior and ultimate failure for wide range corrugated systems. Talbi et al. [15] presented an analytical homogenization model for corrugated cardboard and its numerical implementation in a shell element.

The shape and size of flute have an important effect on the performance of corrugated cardboard. However, there are no strict standards of flute size parameter to achieve the best elasticity and compressive strength of corrugated cardboard. There is also little literature regarding the finite element analysis of flute size. Yuan et al. [16, 17] have developed a model of UV-shaped corrugated cardboard by ANSYS. The results show that the closer the model to the U-shaped flute, the larger the corrugated board strain becomes. It is consistent with the empirical data, which prove the feasibility of finite element analysis method. In this paper, we focus on the investigation of nonlinear finite element analysis of the fluted corrugated sheet in the corrugated cardboard based on software SolidWorks2008. The shape and size of flute will be discussed with the help of SolidWorks and compared with the empirical data.

Table 1: Parameters of linear elastic material [18].

| Name | | Numerical value | Unit |
|---|---|---|---|
| Elastic modulus | $E_x$ | 7600 | MPa |
| | $E_y$ | 4020 | MPa |
| | $E_z$ | 38 | MPa |
| Shear modulus | $G_{xy}$ | 2140 | MPa |
| | $G_{xz}$ | 20 | MPa |
| | $G_{yz}$ | 70 | MPa |
| Poisson's ratio | $V_{xy}$ | 0.34 | — |
| | $V_{xz}$ | 0.01 | — |
| | $V_{yz}$ | 0.01 | — |
| Density | | 404.5 | kg/m$^3$ |

Table 2: Parameters of rigid plate material.

| Name | Numerical value | Unit |
|---|---|---|
| Elastic modulus | $1.0 \times 10^{12}$ | N/m$^2$ |
| Density | $1.0 \times 10^{-8}$ | kg/m$^3$ |
| Poisson's ratio | 0.3 | — |

## 2. Modeling

SolidWorks2008 has powerful structural modeling functions, among which Cosmos/Works is a function module which is specially used to make finite element analysis on structure. The model of common UV-shaped corrugated board is shown in Figure 2. In Figure 2, $L$ is flute length, $H$ is flute height, $h$ is facing paper thickness, $\delta$ is fluting paper thickness, $\theta$ is flute angle, and $r$ is arc radius.

The principal aim of this work is to study the fluted corrugated sheet. So we added a piece of rigid plate with large elastic modulus on upper facing paper (as shown in Figure 3) to eliminate the influence of the facing paper deformation. The maximum stress and strain of the improved model occur in the point in which flute contact with the upper facing paper in all cases. The material parameters of corrugated board model are given in Table 1 [18]. The material parameters of rigid plate model are given in Table 2 from the SolidWorks material library.

## 3. Results and Discussion

*3.1. The Numbers of Flutes in Models.* In order to eliminate the influence of the number of flutes in models, a series

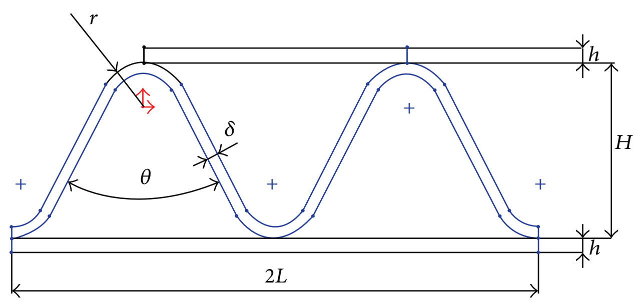


Figure 2: Model of UV-shaped corrugated board.

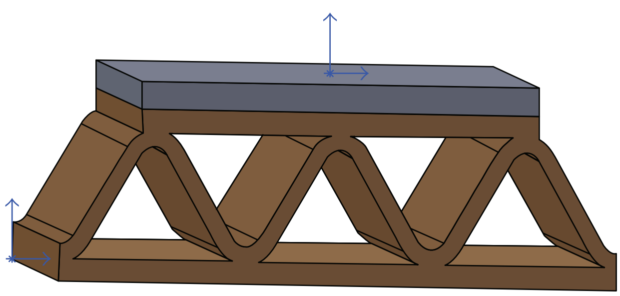

Figure 3: Improved model of UV-shaped corrugated board with rigid plate.

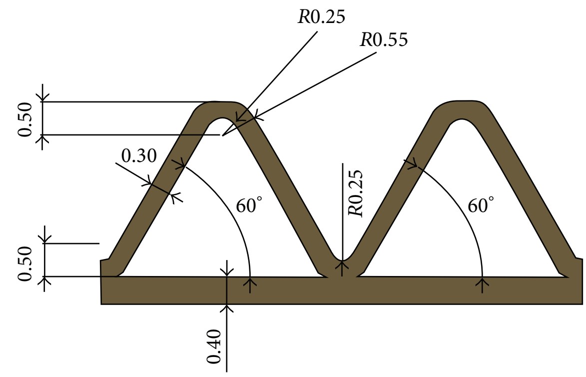


Figure 4: Model of corrugated board with two flutes.

of models with different number of flutes were built and shown in Figure 4. The numbers of flutes in models are 2, 3, 4, and 5. Fixing the bottom of models and then a static pressure test were made with a pressure of 150 Pa on the top floor. Then the stress and displacement contours of models of corrugated board were obtained as shown in Figure 5 (model with three flutes as example). From above calculation, the maximum displacement and maximum stress of the models with different number of flutes were obtained and the results are shown in Figure 6.

From Figure 6, we can see that, with the number of flutes increased, the maximum stress in the models increased and the maximum displacement decreased. While the number of flutes increased to 3 or more, the maximum stress and displacement changed slightly. Therefore, the model of corrugated board with three or more flutes is reliable for stress and displacement measurement. In the coming simulation, the numbers of flutes in the models are all greater than 2.

*3.2. Flute Height $H$.* Effects of flute height $H$ on the mechanical properties of corrugated cardboard model were investigated. A series of models with different flute height $H$ were built and shown in Figure 7. The flute heights $H$ in models are 2, 3, 4, and 5 mm. These models can be roughly classified as A flute (5 mm), C flute (4 mm), B flute (3 mm), and E flute (2 mm). Fixing the bottom of models and then a static pressure test were made with a pressure of 150 Pa on the top floor. Then the maximum displacement and maximum stress of the models with different flute height $H$ were obtained and the results are shown in Figure 8.

From Figure 8, we can see that, with the flute height $H$ increased, the maximum stress in the models decreased and the maximum displacement increased. Therefore, with the flute height $H$ increased, the flat compression strength of corrugated board decreased and cushioning properties of corrugated board increased. As is well known, the cushioning properties of different shapes of corrugated cardboard have the sequence A > C > B > E, and the flat compression strength of corrugated board has the sequence A < C < B < E. Our simulation results are consistent with these conclusions.

*3.3. Arc Radius $r$.* Effects of arc radius $r$ on the mechanical properties of corrugated cardboard model were investigated in this section. A series of models with different arc radius of flute were built and shown in Figure 9. The arc radius $r$ in models are 0, 0.1, 0.2, 0.25, 0.3, 0.35, and 0.4 mm. Fixing the bottom of models and then a static pressure test were made with a pressure of 150 Pa on the top floor. Then the maximum displacement and maximum stress of the models with different arc radius were obtained and the results are shown in Figure 10.

From Figure 10, we can see that, with the arc radius of flute increased, the maximum stress in the models decreased and the maximum displacement increased. It means that when the arc radius $r$ increases the flat compression properties get worse and the cushioning properties get better. In fact, the smaller the arc radius, the closer the model to the V-shaped flute; the larger the arc radius, the closer the model to U-shaped flute. The simulation result also verified that the flat compression properties of V-shaped flute corrugated board are better than that of the U-shaped flute corrugated board and its cushioning properties are worse than that of the U-shaped flute.

Actually, the triangle is the most stable structure. It is difficult to deform when a force was applied at the vertex of a triangle. But this structure is not suitable for the cushioning design. As the arc radius $r$ increases, the maximum displacements of the structure increase. So the stress can be dispersed to other parts rather than concentrating on one point. In this situation the cushioning properties of corrugated board get better to protect goods. In order to meet the needs of

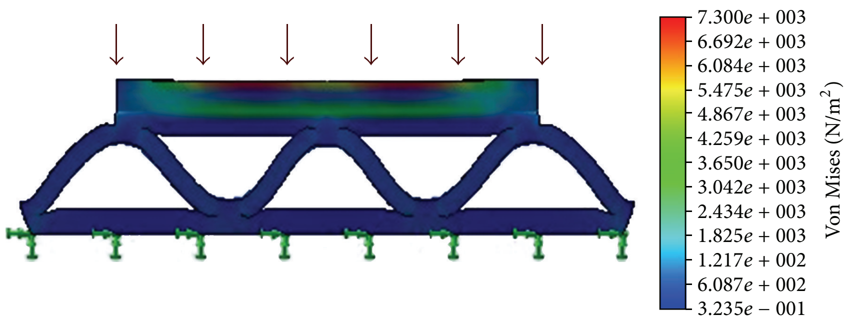


(a) Stress contours

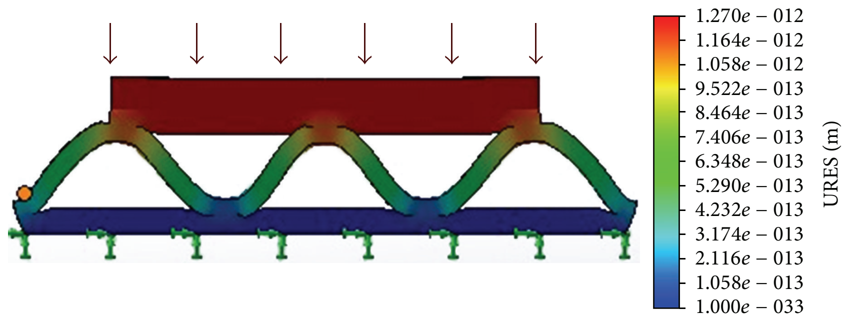


(b) Displacement contours

FIGURE 5: The stress and displacement contours of models of corrugated board with three flutes.

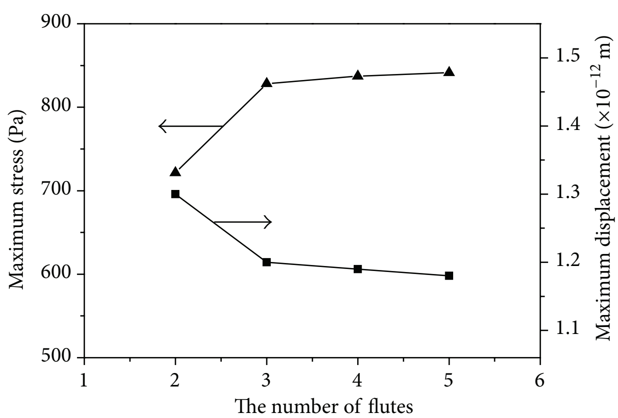


FIGURE 6: Maximum stresses and maximum displacements of corrugated board models with different number of flutes.

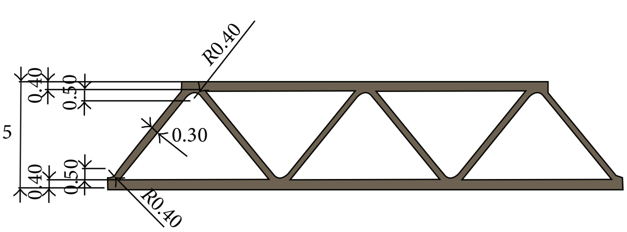


FIGURE 7: Model of corrugated board with flute height $H$ of 5 mm.

packaging cushioning design, we should determine the arc radius $r$ according to the actual packaging requirements.

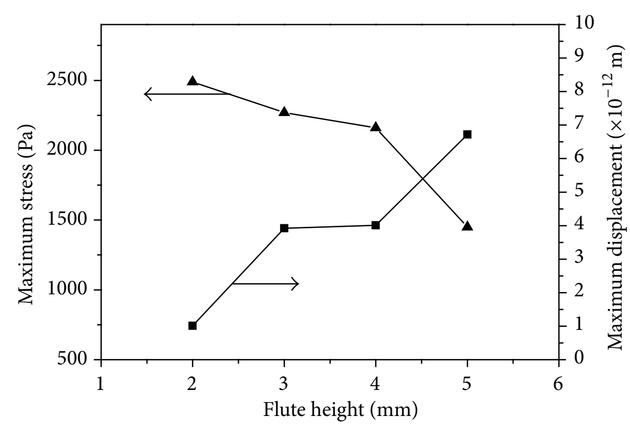


FIGURE 8: Maximum stresses and maximum displacements of corrugated board models with different flute height.

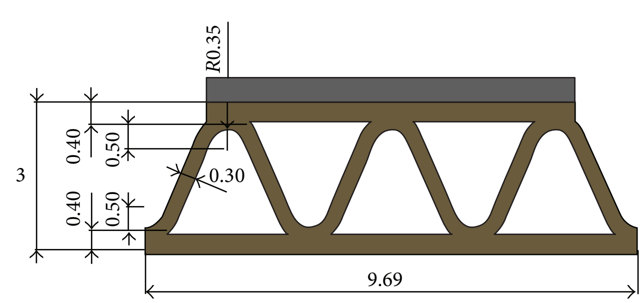


FIGURE 9: Model of corrugated board with arc radius of 0.35 mm.

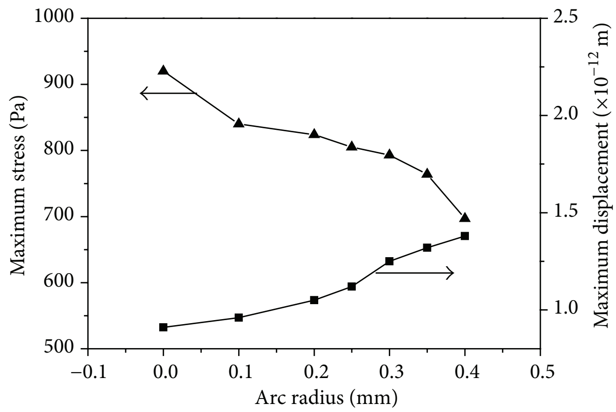


FIGURE 10: Maximum stresses and maximum displacements of corrugated board models with different arc radius of flute.

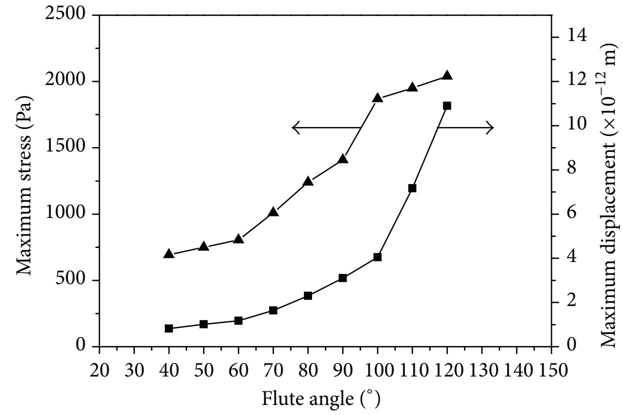


FIGURE 12: Maximum stresses and maximum displacements of corrugated board models with different flute angle $\theta$.

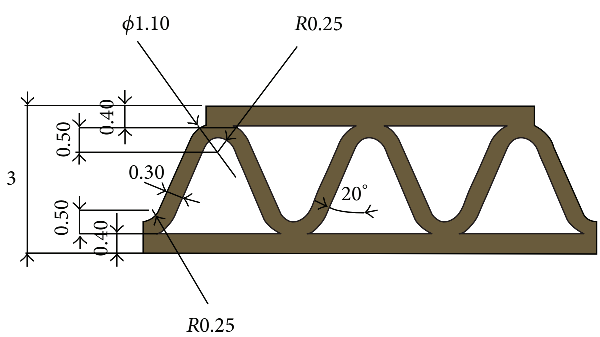


FIGURE 11: Model of corrugated board with flute angle of 40°.

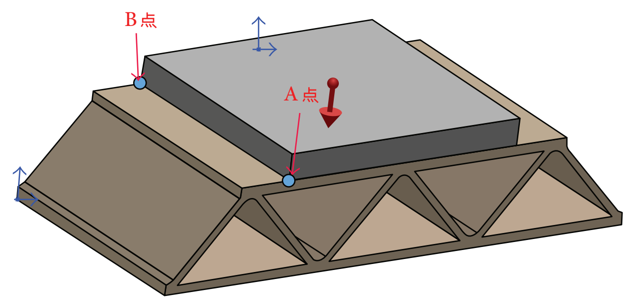


FIGURE 13: The drop test model with different flute height.

*3.4. Flute Angle $\theta$.* Effects of flute angle $\theta$ on the mechanical properties of corrugated cardboard model were investigated in this section. A series of models with different flute angle $\theta$ were built and shown in Figure 11. The flute angles $\theta$ in models are 40, 50, 60, 70, 80, 90, 100, 110, and 120°. Fixing the bottom of models and then a static pressure test were made with a pressure of 150 Pa on the top floor. Then the maximum displacement and maximum stress of the models with different flute angle $\theta$ were obtained and the results are shown in Figure 12.

From Figure 12, we can see that, with the increase of the flute angle $\theta$, the maximum stress and maximum displacement in the models increase nonlinearly. The maximum stress and maximum displacement change slowly when $\theta$ is less than 60° and then increase sharply when $\theta$ is larger than 60°. In addition, the number of flute per unit length increases as the $\theta$ decreases, and it means that the corrugated board needs more materials. Therefore, the optimal flute angle $\theta$ could be 60° for corrugated board. According to the Chinese national standards "Corrugated board and standard test method" (GB6544~6548-86), the UV-shaped flute corrugated board should be 60° in the manufacture process. The simulation result is consistent with the standards of corrugated board.

*3.5. Drop Test*

*3.5.1. Flute Height H.* Both primary (consumer) packages and shipping containers have a risk of being dropped or being impacted by other items. Package integrity and product protection are important packaging functions. Drop tests are conducted to measure the resistance of packages and products to controlled laboratory shock and impact. Drop testing also determines the effectiveness of package cushioning to isolate fragile products from shock.

Effects of flute height $H$ on the dynamic mechanical properties of corrugated cardboard model in the drop test based on Cosmos/Works were investigated. A series of models with different flute height $H$ were built and shown in Figure 7. The flute heights $H$ in models are 2, 3, 4, and 5 mm. The drop test model was shown in Figure 13. A simplified model of corrugated board and goods on the upper board were investigated. Drop height is 0.3 m, initial velocity is 0 m/s, acceleration of gravity is 9.81 m/s$^2$, and impact time is 600 $\mu$s. The material of the object on the upper board is Acrylonitrile Butadiene Styrene (ABS) and the mass is $1.224 \times 10^{-4}$ kg. Then the stress and displacement contours of models of corrugated board were obtained and shown in Figure 14 (model with flute height $H$ of 5 mm). In order to investigate the stress of goods on the upper board in the drop test, we selected 2 points (A and B point as shown in Figure 13) from the model as the object of study. Then the time-dependent

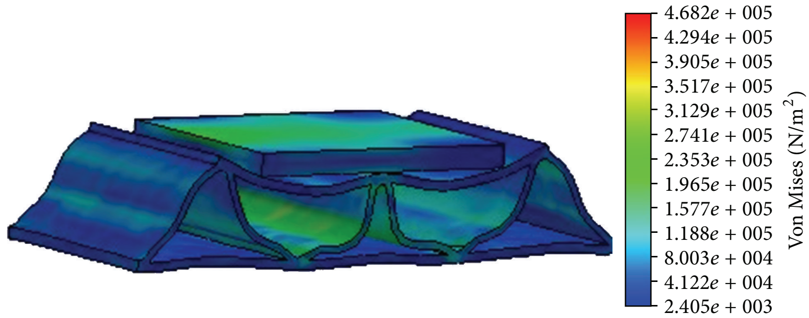


(a) Stress contours

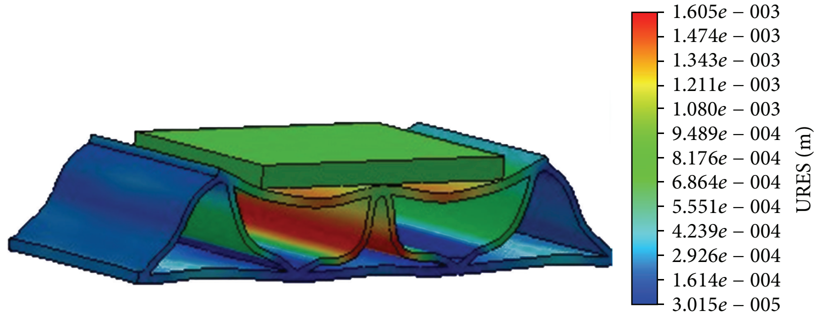


(b) Displacement contours

Figure 14: The stress and displacement contours of model with flute height $H$ of 5 mm in drop test.

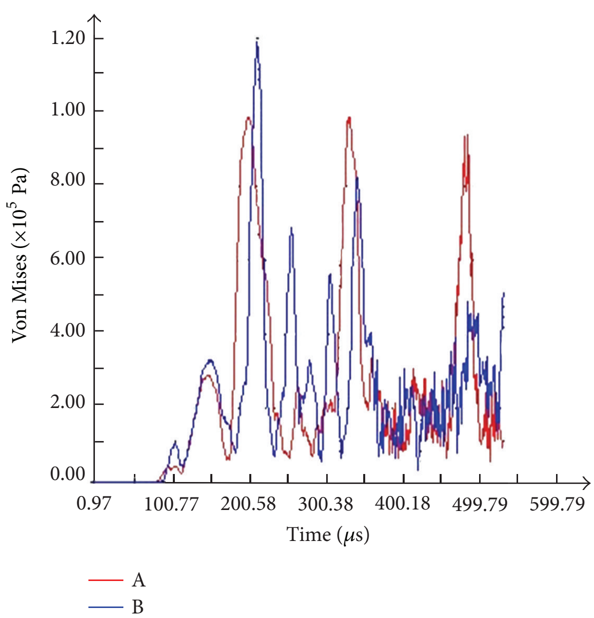


Figure 15: Time-dependent stress of A, B point in drop test (model with flute height $H$ of 5 mm).

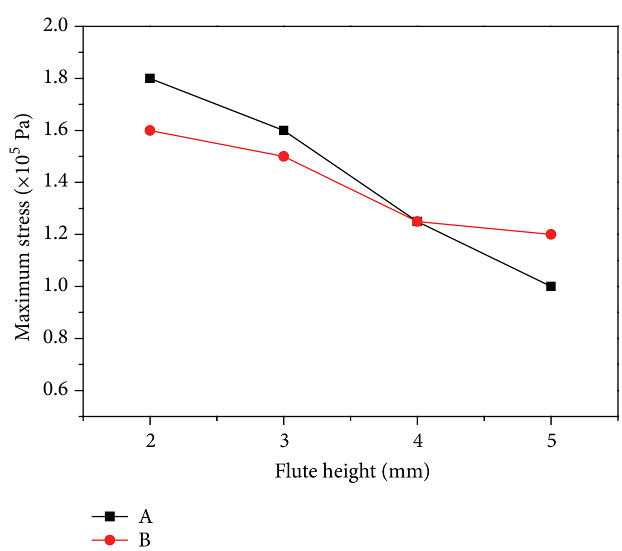


Figure 16: Maximum stress of A, B point in the models with different flute height $H$ in the drop test.

stress of A, B point in the drop test was obtained and shown in Figure 15 (model with flute height $H$ of 5 mm). From above simulation, the maximum stresses of A, B point in the models with different flute height $H$ in the drop test were obtained and the results are shown in Figure 16.

From Figure 16, we can see that, with the increase of flute height $H$, the maximum stress of goods on the upper board in the drop test decreased. Therefore, with the increase of flute height $H$, the cushioning properties of corrugated board increased. This conclusion is consistent with the conclusions of Section 3.2.

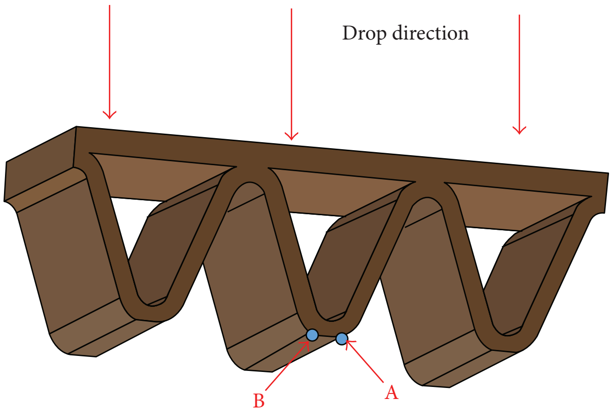


Figure 17: The drop test model with different flute angle $\theta$.

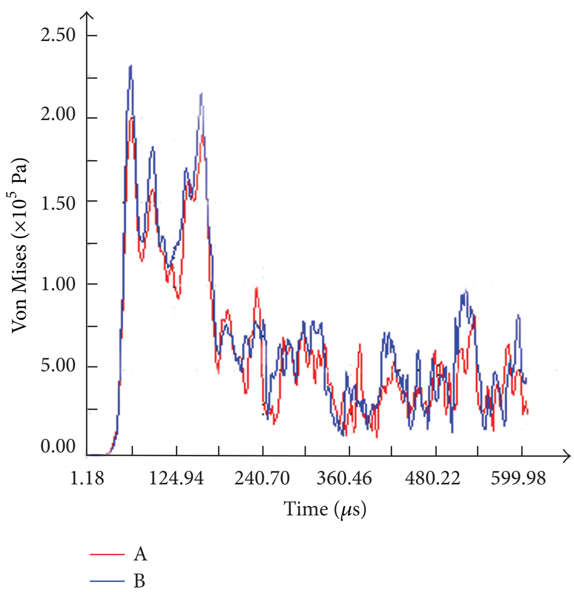


Figure 18: Time-dependent stress of A, B point in drop test (model with flute angle $\theta$ of 40°).

*3.5.2. Flute Angle $\theta$.* Effects of flute angle $\theta$ on the dynamic mechanical properties of corrugated cardboard model in the drop test based on Cosmos/Works were investigated. A series of models with different flute angle $\theta$ were built and shown in Figure 11. The flute angles $\theta$ in models are 40, 50, 60, 80, and 100°. The drop test model was shown in Figure 17. Drop height is 0.3 m, initial velocity is 0 m/s, acceleration of gravity is 9.81 m/s$^2$, and impact time is 600 $\mu$s. The stress distribution of corrugated cardboard was obtained and we have found that the maximum stress occurs in the point which fluted corrugated sheet contact with the ground in all cases. So we selected 2 points (A and B point as shown in Figure 17) from the model as the object of study in the drop test. Then the time-dependent stress of A, B point in the drop test was obtained and shown in Figure 18 (model with flute angle $\theta$ of 40°). From above simulation, the maximum stresses of A, B

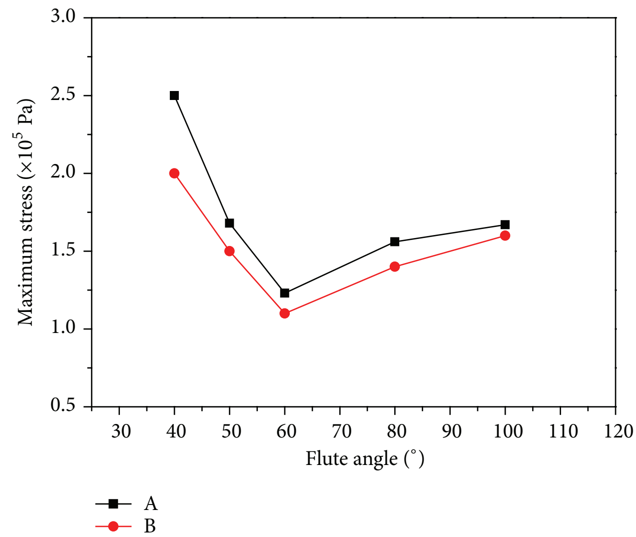


Figure 19: Maximum stress of A, B point in the models with different flute angle in the drop test.

point in the models with different flute angle $\theta$ in the drop test were obtained and the results are shown in Figure 19.

From Figure 19, we can see, that with the increase of flute angle, the maximum stress of the model in the drop test decreases firstly and then increases. The maximum stress of the corrugated board bears is smallest when the flute angle $\theta$ reaches 60°. The reason is that the stress of the corrugated board could be dispersed to the flute structure efficiently and then reduces the maximum stress of the corrugated board in drop test. Therefore, the optimal flute angle $\theta$ could be 60° for corrugated board. This conclusion is consistent with the conclusions of Section 3.4.

## 4. Conclusions

The shape and size of flute have an important effect on the performance of corrugated cardboard. In this paper, the nonlinear finite element analysis of the fluted corrugated sheet in the corrugated cardboard based on software SolidWorks2008 was investigated. The obtained conclusions are as follow.

(1) According to the static pressure test, with the flute height $H$ increased, the maximum stress in the models decreased and the maximum displacement increased.

(2) According to the static pressure test, with the arc radius of flute increased, the maximum stress in the models decreased and the maximum displacement increased.

(3) According to the static pressure test, with the increase of the flute angle $\theta$, the maximum stress and maximum displacement in the models increase nonlinearly. The optimal flute angle $\theta$ could be 60° for corrugated board.

(4) According to the drop test, with the increase of flute height $H$, the maximum stress of goods on the upper board in the drop test decreased.

(5) According to the drop test, with the increase of flute angle, the maximum stress of the model decreases firstly and then increases. The maximum stress of the corrugated board bears is smallest when the flute angle $\theta$ reaches $60^{\circ}$. Therefore, the optimal flute angle $\theta$ could be $60^{\circ}$ for corrugated board.

All the conclusions are consistent with experimental data or product standards.

## Conflict of Interests

The authors declare that there is no conflict of interests regarding the publication of this paper.

## Acknowledgments

This work was financially supported by the National Natural Science Foundation of China (51206148, 51106140), Major Programs of Sci & Tech, Department of Science and Technology of Zhejiang Province (2008C12062, 2013C03017-4), and Zhejiang Provincial Natural Science Foundation of China (Y1110642, Y407311). The authors are thankful for the financial support of Zhejiang Provincial Key Disciplines "Pulp and Paper Engineering."

## References

[1] M. E. Biancolini, C. Brutti, and S. Porziani, "Corrugated board containers design methods," *International Journal of Computational Materials Science and Surface Engineering*, vol. 3, no. 2-3, pp. 143–163, 2010.

[2] http://en.wikipedia.org/wiki/Corrugated_fiberboard.

[3] M. Tuomela, M. Vikman, A. Hatakka, and M. Itävaara, "Biodegradation of lignin in a compost environment: a review," *Bioresource Technology*, vol. 72, no. 2, pp. 169–183, 2000.

[4] A. C. Gilchrist, J. C. Suhling, and T. J. Urbanik, "Nonlinear finite element modeling of corrugated board," in *ASME Joint Applied Mechanicals and Materials Division Meeting*, pp. 101–106, 1998.

[5] D. Twede and S. E. M. Selke, *Cartons, Crates and Corrugated Board: Handbook of Paper and Wood Packaging Technology*, DEStech, 2005.

[6] T. J. Lu, C. Chen, and G. Zhu, "Compressive behaviour of corrugated board panels," *Journal of Composite Materials*, vol. 35, no. 23, pp. 2098–2126, 2001.

[7] T. Nordstrand, "Analysis and testing of corrugated board panels into the post-buckling regime," *Composite Structures*, vol. 63, no. 2, pp. 189–199, 2004.

[8] U. Nyman and P. J. Gustafsson, "Material and structural failure criterion of corrugated board facings," *Composite Structures*, vol. 50, no. 1, pp. 79–83, 2000.

[9] M. Daum, D. Darby, G. Batt, and L. Campbell, "Application of the stress-energy method for generating corrugated board cushion curves," *Journal of Testing and Evaluation*, vol. 41, no. 4, pp. 590–601, 2013.

[10] J. Viguié, P. J. J. Dumont, L. Orgéas, P. Vacher, I. Desloges, and E. Mauret, "Surface stress and strain fields on compressed panels of corrugated board boxes: an experimental analysis by using digital image stereocorrelation," *Composite Structures*, vol. 93, no. 11, pp. 2861–2873, 2011.

[11] M. E. Biancolini and C. Brutti, "Numerical and experimental investigation of the strength of corrugated board packages," *Packaging Technology and Science*, vol. 16, no. 2, pp. 47–60, 2003.

[12] M. E. Biancolini, "Evaluation of equivalent stiffness properties of corrugated board," *Composite Structures*, vol. 69, no. 3, pp. 322–328, 2005.

[13] I. Conde, B. García, E. Liarte, and M. A. Jiménez, "Analysis of adhesive joints in corrugated board under shear loading," *International Journal of Adhesion and Adhesives*, vol. 38, pp. 50–57, 2012.

[14] R. Haj-Ali, J. Choi, B.-S. Wei, R. Popil, and M. Schaepe, "Refined nonlinear finite element models for corrugated fiberboards," *Composite Structures*, vol. 87, no. 4, pp. 321–333, 2009.

[15] N. Talbi, A. Batti, R. Ayad, and Y. Q. Guo, "An analytical homogenization model for finite element modelling of corrugated cardboard," *Composite Structures*, vol. 88, no. 2, pp. 280–289, 2009.

[16] W. Yuan, M. G. Zhang, Z. D. Liao et al., "Corrugated board flute-shaped finite element analysis and optimization," *Applied Mechanics and Materials*, vol. 477-478, pp. 1205–1209, 2014.

[17] W. Yuan, J. X. Sun, G. M. Zhang et al., "Corrugated board UV flute-shaped structure size optimization design based on the finite element," *Applied Mechanics and Materials*, vol. 469, pp. 213–216, 2014.

[18] H. Guang-jun, H. Xiang, and F. Wei, "Finite element modeling and buckling analysis of corrugated box," *Packaging Engineering*, vol. 30, no. 3, pp. 34–35, 2009.